ELSEVIER

Tectonophysics 356 (2002) 253–273

TECTONOPHYSICS

www.elsevier.com/locate/tecto

Three-dimensional laboratory modelling of rifting: application to the Baikal Rift, Russia

A. Chemenda [a,*], J. Déverchère [b], E. Calais [c]

[a] *Géosciences Azur, UMR 6526, Université de Nice-Sophia Antipolis, 250 Rue Albert Einstein-Sophia Antipolis, 06560 Valbonne, France*
[b] *Géosciences Azur, UMR 6526, Université Pierre et Marie Curie, Quai de la Darse-BP 48, 06235 Villefranche-sur-Mer, France*
[c] *Department of Earth and Atmospheric Sciences, Purdue University, West Lafayette, IN 47907-1397, USA*

Received 6 September 2001; accepted 5 July 2002

Abstract

Continental rifting is treated as a mechanical instability developing under horizontal tectonic tension. The instability results in strain localization and the formation of a neck, which is interpreted as a rift zone. At the scale of the whole lithospheric plate, this process occurs in plane-stress conditions and can therefore be modelled to a first approximation by a one-layer plate whose properties represent integral (over thickness) properties of the real lithosphere. We have designed a scaled experimental single-layer lithosphere model having elasto-plastic rheology and lying upon a liquid substratum to study its behaviour under axial horizontal tension. In a homogeneous plate, the instability develops along a linear zone oriented at an angle of $\sim 60^\circ$ to the tension axis. This orientation is preserved even when the divergent displacement of the plate boundaries is not plain-parallel but rotational. In the latter case, the strain localization zone is rapidly propagating. When the plate length to width ratio is less than ~ 2.5, the necking develops along two branches conjugated at an angle of about 120°, which is frequently observed in actual rift systems. If the model contains a local weak zone (hot spot or fault zone), the rift junction is located at this zone. In the lithospheric models comprising strong (cratonic) and weak segments, strain localization depends on the configuration of the boundary between different lithospheres. The necking starts to form within the weak segment in the vicinity of the cratonic promontories and propagates in opposite directions again at an angle of ca. 60° to the tension axis. In the models containing both a strong lithosphere and local weak zones, the rift configuration depends on their shape and relative positions, with necking always going through the weak zones. In a set of models, we have reproduced the geometry of the boundary between the Siberian craton and the thermally much younger (~ 100 Ma) Sayan–Baikal lithosphere in the Baikal rift area. In these models, we were able to obtain the well-known three-branch configuration of the Baikal rift system only by introducing a weak zone in the area of Lake Baikal. Such a zone simulates the Paleozoic suture existing in this area. As in nature, two wide outer branches (eastern and western) are oblique to the regional tension axis, whereas the central one is narrow and orthogonal to the tension direction. In nature and in the model, rifting starts in the central branch corresponding to Lake Baikal. The modelling also predicts the formation of a fourth oblique $\sim$ NS-trending branch to the south of Baikal. Although poorly expressed in the field, this branch has some seismotectonic and magmatic manifestations. The orientations of all four branches with respect to each other and with respect to the regional tension direction are remarkably similar in nature and in the model.

Keywords: Rifting; Geodynamics; Physical modelling; Mechanics of the lithosphere; Baikal; Strain localisation

* Corresponding author. Tel.: +33-4-92-94-26-61; fax: +33-4-92-64-26-10.
E-mail address: chem@geoazur.unice.fr (A. Chemenda).

0040-1951/02/$ - see front matter © 2002 Elsevier Science B.V. All rights reserved.
PII: S0040-1951(02)00389-X

1. Introduction

Continental rifts occur under tectonic extension of the lithosphere. The numerous discussions about active versus passive rifting mechanisms generally lead to the conclusion that both processes exist and probably work simultaneously in a rift zone, with one or another mechanism dominating (Forsyth and Uyeda, 1975; Morgan and Baker, 1983; Ziegler, 1992; Olsen, 1995; Ruppel, 1995). There is a general agreement that rifts basically represent zones of extensional strain localization, although the role of non-mechanical processes (such as mineralogical transformations, e.g., Artyushkov, 1981) in the crustal thinning and formation of the rift valleys remains unclear. Strain localization within the lithosphere depends on its rheology, boundary and initial conditions. This process has been widely modelled using both experimental (e.g., Faugères et al., 1986; Allemand et al., 1989; Shemenda, 1984; Tron and Brun, 1991; McClay and White, 1995; Brun and Beslier, 1996; Benes and Davy, 1996; Bonini et al., 1997) and numerical (e.g., Buck, 1991; Martinod and Davy, 1992; Hassani and Chéry, 1996; Hopper and Buck, 1996, 1998; Houseman and Molnar, 1997; Burov and Poliakov, 2001) techniques. These studies show that strain localization results in lithospheric necking, either symmetrical with respect to a vertical plane (Buck, 1991; Brun and Beslier, 1996) or asymmetrical in the models where the lithospheric material is allowed to fail (or is prefailed) along an inclined normal (detachment) fault (Faugères et al., 1986; Dunbar and Sawyer, 1989; Allemand et al., 1989; Malkin and Shemenda, 1991; Lesne et al., 2000). The details of the deformation pattern depend on the rheological structure of the lithosphere that can contain one, two or more weak layers, following adopted petrological models, geotherm and wet or dry rheology (Ranalli and Murphy, 1987; Tommasi et al., 1995). Geological heritage such as preexisting faults, weak (hot) and/or strong (cold) zones in the lithosphere, and its mechanical anisotropy also appear to play a major role (Dunbar and Sawyer, 1989; Malkin and Shemenda, 1991; Vauchez et al., 1997, 1998; Lesne et al., 2000).

Both rheological and mechanical structures of the lithosphere are poorly constrained, while 2-D numerical models show that the deformation of the lithosphere in cross-section is extremely sensitive to its rheological stratification (e.g., Burov and Poliakov, 2001, and references therein) There is therefore a large freedom in "adjusting" complex models to fit one or another set of observations. On the other hand, 3-D aspects of the lithospheric strain localization are almost unexplored, whereas the majority of the rifts (Baikal in particular) represent essentially 3-D structures. Stresses generated within the rigid (elastic) lithospheric envelope in the presence of various types of heterogeneities (faults, strong and week zones) may result in a strain localization (plastic failure) pattern that cannot be predicted by 2-D models. The cross-section deformation will be defined by this 3-D pattern and thus cannot be thoroughly understood through 2-D models.

In this paper, we present results from 3-D experimental modelling of uniaxial horizontal extension of a simple one-layer plastic lithosphere designed to understand a first-order lithospheric-scale mechanics of rifting. We study strain localization within a heterogeneous plate consisting of both strong and thick (cratonic) and thermally younger lithospheres. The experiments show that strain localization always occurs within the weak lithosphere. The localization is initiated near the cratonic promontories and then propagates away. The geometry of the final "rift system" depends on the configuration of the boundary between strong and weak lithospheres, thus showing the importance of a 3-D lithosphere structure. Local weak lithospheric zones also strongly affect the strain localization process by "attracting" the rifts. We simulated two types of weak zones corresponding to the fault zones and to the hot spots and showed that the rifts always go through the hot spots and generally initiate on the fault zones. By introducing both strong and weak zones into the model, we attempt to approach the actual situation in the Baikal rift system.

2. Modelling set up

The experimental technique, analogue materials and similarity criteria are similar to those described by Shemenda (1984) and Malkin and Shemenda (1991) and are briefly presented below. The modelling scheme is shown in Fig. 1. The lithosphere is modelled by elasto-plastic material with strain weakening

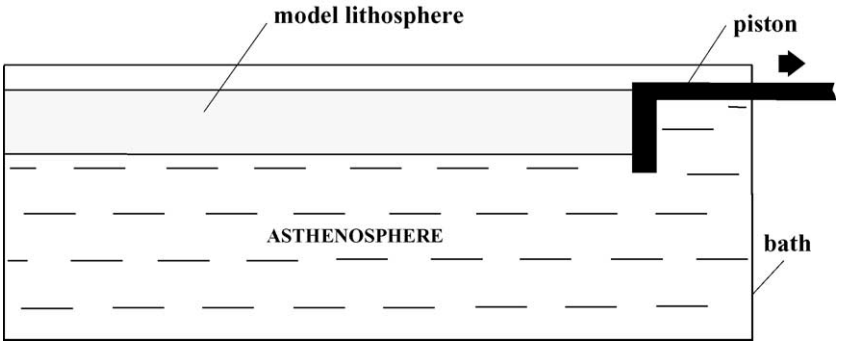

Fig. 1. Modelling set up scheme.

(Fig. 2) made of compositional systems consisting of alloys of solid hydrocarbons, mineral oils, finely grounded powders and small quantities of surface-active substances (Shemenda, 1994). The asthenosphere is modelled by pure water. The rectangular lithosphere model, floating in the water, is "welded" in this floating state to the piston and to the opposite wall of the experimental installation. The lateral borders of the "lithosphere" are free and do not touch the bath walls. Extension of the lithosphere is produced by a piston. The similarity criteria met in this modelling are:

$$\tau_s/(\rho_l g H) = \text{const}; \quad E/\tau_s = \text{const};$$
$$\rho_l/\rho_a = \text{const}; \quad Vt/H = \text{const}, \qquad (1)$$

where τ_s is the lithospheric shear yield limit; E is the effective lithospheric elasticity modulus; ρ_l and ρ_a are the densities of the lithosphere and the asthenosphere, respectively; H is the lithosphere thickness; g is the acceleration of gravity; V is the rate of extension; and t is the time. The first criterion is the most important in this modelling as it scales the gravity forces responsible in particular for the relief formation. The geological time t is scaled via the displacement (amount of extension) $\Delta l = Vt$ (see the last condition in (1)). We have assumed the following parameter values for the prototype (nature): $\tau_s = 170$ MPa; $E = 17$ GPa; $\rho_l = \rho_a = 3.3 \times 10^3$ kg/m^3; $H = 10^5$ m; $V = 1$ cm/year. The conditions in (1) are satisfied for the following model parameter values adopted in the experiments presented below: $\tau_s = 9.5$ Pa; $E \approx 10^4$ Pa; $\rho_l = \rho_a = 0.94 \times 10^3$ kg/m^3; $H = 1.5 \times 10^{-2}$ m (average value); $V = 2 \times 10^{-3}$ m/s.

Both homogeneous and heterogeneous lithosphere models were tested. The whole model was made of the same material whose yield limit is highly temperature dependent and drops with temperature increase. The experiments were conducted under the temperature of about 40 °C when the lithosphere model parameters have values indicated above. Temperature increase by 2° results in about two times reduction of the lithosphere yield limit. Temperature decrease by 2° results in ~2.5 times strength increase. The old

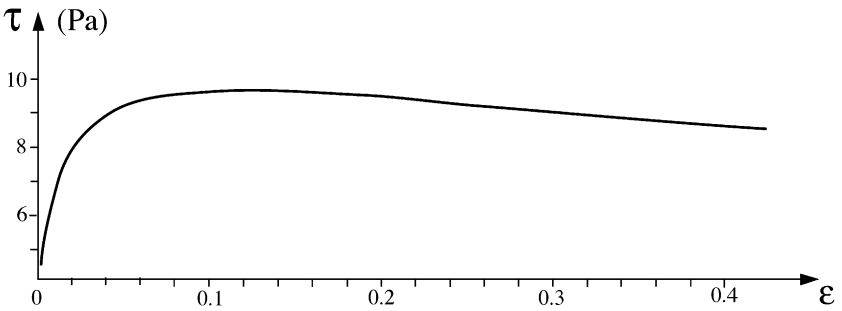

Fig. 2. Stress (τ)/strain (ε) diagram for the model material at $\dot{\varepsilon} = 7 \times 10^{-2}$ s^{-1} and temperature $T = 40$ °C (shear testing).

(cratonic) lithosphere was modelled by a thicker plate. A thicker plate has higher effective strength. To further increase the strength contrast between "normal" and "cratonic" lithospheres, we maintained the surface of the latter at a lower temperature of ~ 38 °C. In fact, it was found that if the plate thickness contrast is greater than ~ 20%, the temperature decrease (yield limit increase) of the thicker lithosphere does not affect the model deformation: The "cratonic lithosphere" remains undeformed, and the thinner model segment deforms independently on the strength contrast value.

The weak zones were introduced in the lithosphere model in three different ways: In a chosen area we: (a) pierced with a needle many times or cut the "lithosphere" through its whole thickness; (b) scraped the material from the plate surface and/or bottom to locally reduce its thickness and hence effective strength; and (c) produced local additional heating of the model surface. In the latter case, an electric heater of a given (circular or elongated) shape was fixed at about 2 mm from the model surface. It was regulated to maintain the model surface temperature (controlled by a microthermocouple) at 42–43 °C. The local heating lasted about 10–15 min and was produced just before the model deformation. If the model weakening was sufficient, the all weakening techniques led to basically the same result: The deformation was always localised at a weak zone and then propagated away independ-

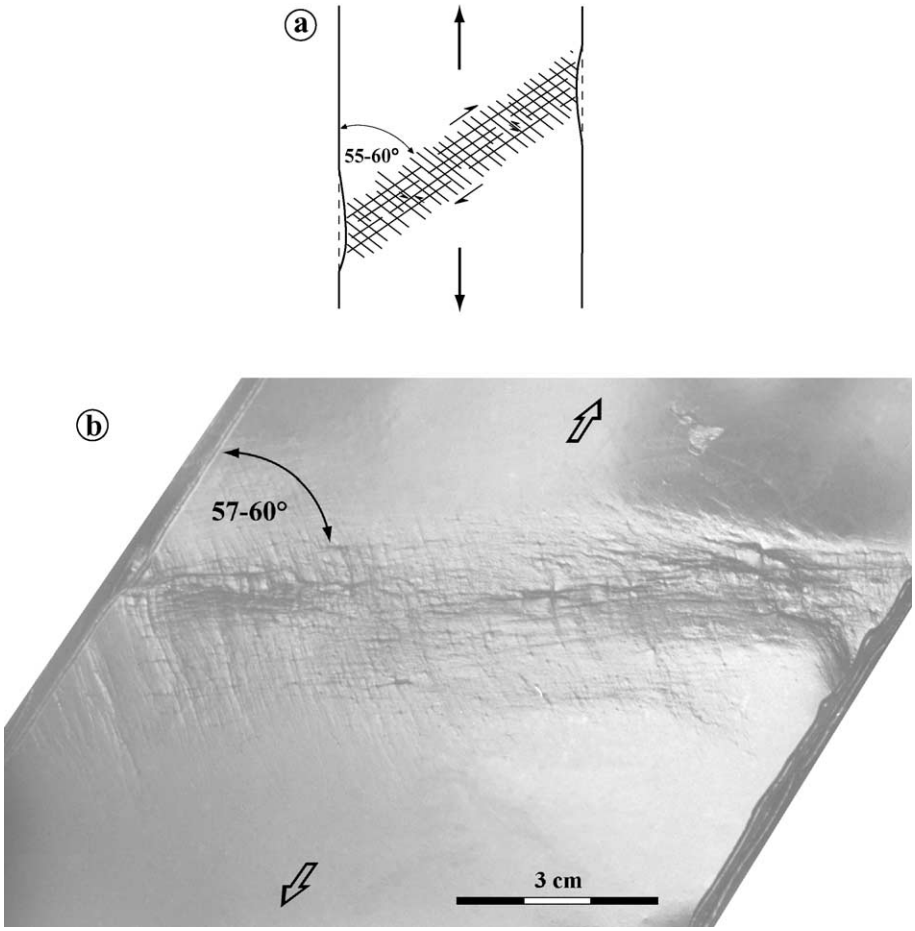

Fig. 3. Deformation pattern observed at the model surface. (a) Scheme of the slip (Luders)-lines; (b) oblique view of the model surface (experimental photograph).

ently on the way the plate is weakening. When the weakening was very small, it did not affect the deformation; the model deformed as if it were homogeneous. We did not aim to determine exactly the threshold weakening value but found that about 20% plate thinning is already sufficient for the deformation to be localised on a weak zone. About 10–15 min of local heating also was sufficient to change the model deformation pattern. We conclude therefore that ~ 10 min heating produces about 20% plate weakening.

3. Summary of previous experiments

We first summarize the main experimental results reported by Shemenda (1984) and Malkin and Shemenda (1991) by completing them with new similar experimental tests.

3.1. Strain localization within a homogeneous plate

An initially homogeneous experimental lithosphere model subjected to an axial tension first undergoes uniform lengthening. Then the deformation localizes along a linear zone with a width comparable to the plate thickness (Figs. 3 and 4). At the surface, the strain localization zone (the rift) is manifested by two slip-line (Luders line) families oriented at the angle of about $\psi = \pm \sim 60^\circ$ to the tension axis and by the forming valley. The orientation of the strain localization zone coincides with one slip-line family, with another family being died just after the formation. The localization can occur along either direction at $+60^\circ$ or -60° to the tension axis with equal probability (this angle varies from $\sim 55^\circ$ to more than 62° from one experiment to another). The deformation evolution across the "rift" is characterized by the formation of a necking symmetrical with respect to the vertical and asymmetrical with respect to the horizontal (Fig. 4). The asymmetry occurs starting from some stage of extension that depends on the lithospheric strength τ_s or more exactly on the value of the first criteria in (1): $\Omega = \tau_s/(\rho_l g H)$. When Ω (or τ_s) is very small, the plate thinning occurs practically only from below due to the isostatic recovering of the forming rift valley (this feature is very shallow). When Ω (or τ_s) is too high (not scaled to the gravity forces), the neck is symmetrical (Shemenda, 1984; Shemenda and Groholsky, 1994). The latter situation corresponds to the experiments with homogeneous steel sheets subjected to a uniaxial tension (Nadai, 1950). In these experiments, similar linear necks oriented at an angle of $\sim 60^\circ$ to the tension direction were obtained. The necks, however, were symmetrical with respect to the median line of the sheets as the Ω value was very large (large τ_s and small H).

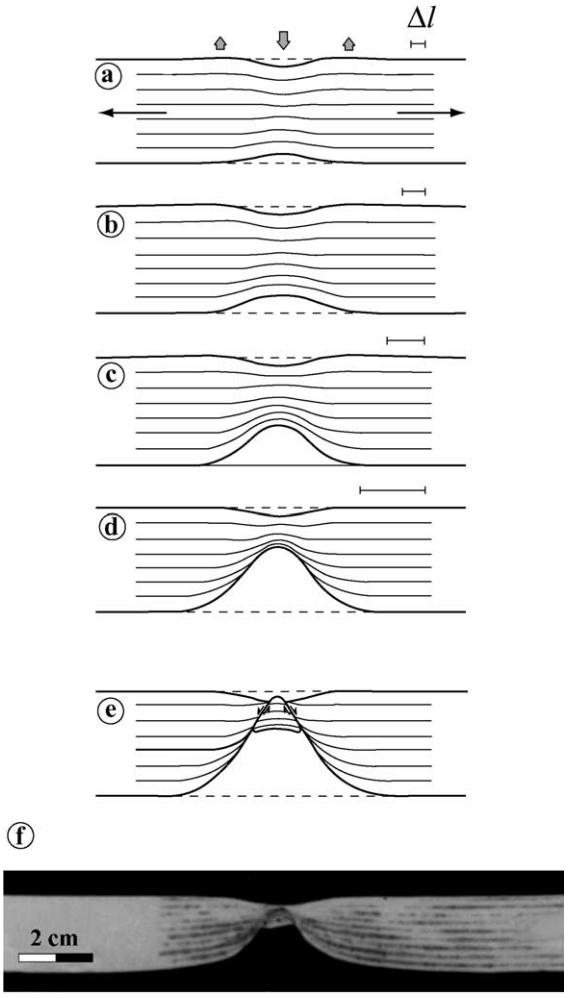

Fig. 4. Evolution of the necking in cross-section (a–e) and experimental photograph of the final stage (f). Thick arrows in (a) show vertical displacement of the model surface. Uplift of the rift shoulders is observed only at the initial stages of the necking. Its amplitude is very small in the model, less than 1 mm (a few kilometres in nature).

3.2. Effect of preexisting faults

In this set of experiments, the initially homogeneous plate was cut vertically in its upper part before extension (Fig. 5a). The minimal cut depth was 1–2 mm, which corresponds in nature to a few to several kilometres. When the cut is parallel to the stretching direction, the plate deformation occurs as if no cut exists, i.e., in the same way as shown in Fig. 3 even when the cut is made throughout the whole plate thickness. When the cut shown in Fig. 5 is oblique to the tension axis, the deformation occurs as follows: The plate first undergoes some thinning at the base under the cut with opening and slight downward propagation of the cut in the upper part of the model (Fig. 5b). Simultaneously, a shear displacement is observed at the surface along the cut. In the cross-section perpendicular to the cut, two conjugated narrow shear zones are forming, which separate a rising wedge (Fig. 5b). Failure of the material along one of these zones makes the deformation asymmetrical and results in the formation of a lithospheric

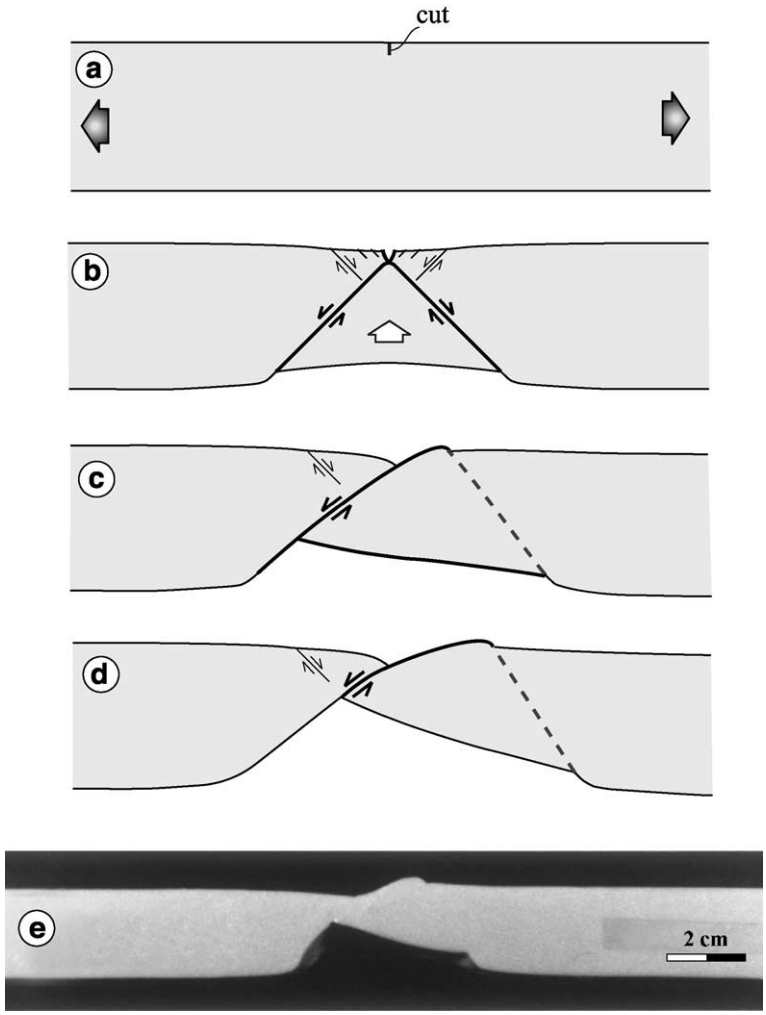

Fig. 5. Strain localization in the model with shallow vertical cut oriented at an angle of $<90^\circ$ to the stretching direction: (a–d) successive stages of deformation in cross-section orthogonal to the cut; (e) experimental photograph of the final stage.

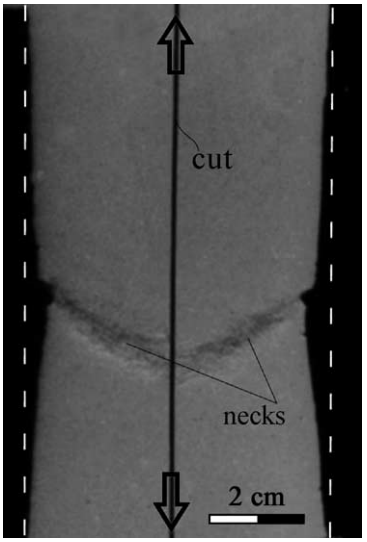

Fig. 6. Photograph from above of the model with vertical cut through the whole plate thickness parallel to the tension axis.

detachment fault, with slip along the other zone being stopped (Fig. 5c and e). When the initial cut is inclined, the deformation is simpler: The cut propagates through the whole plate thickness at a dip angle close to 45°, resulting straightaway in the formation of a detachment fault. Such a process occurs even when the surface trace of the cut is perpendicular to the tension axis.

When instead of a single cut a fault zone is created by making a number of closely located cuts, the strain localizes along such a zone even when the individual cuts are vertical and perpendicular to the tension axis. The deformation pattern depends on the width and dip of the fault zone as well as on the density of the cuts, but it basically corresponds to a plate thinning within the fault zone.

In Fig. 6, we show one more experiment where a vertical individual cut has been made parallel to the tension axis. One can see two rift segments oriented at about $+60°$ and $-60°$ to the tension direction (to the cut) and conjugated at an angle of $\sim 120°$. In some other experiments conducted under the same conditions, we obtained only a single rift (as in Fig. 3) crossing the cut as if it were not existed. This shows that two deformation modes are possible under these conditions, but we did not investigate whether they are equally likely or not.

3.3. Effect of the plate length/width ratio and of a local weak zone

A single strain localization zone occurs in the homogeneous models only when ratio $L/d>2.5$ (L is the plate length in the tension direction, and d is its width). If L/d ratio is smaller, the deformation localizes "hardly" and produces more complicated pattern, like that shown in Fig. 7. At the beginning of extension, slip-lines of both families appear in different places of the model, accompanying the initiation of strain localization at these places. Then the deformation stops everywhere except along two conjugated "rift" segments oriented at about 120° to each other. Within the homogeneous plate, the rift junction can occur at various places, and not necessarily in the middle of the plate. If the model contains a local weak zone, the rift junction is located at this zone (Malkin and Shemenda, 1991). The weak zone can correspond either to the fault zone or to the hot spot, which is often the location of the rift junction at an angle close to 120° (e.g., Burke and Dewey, 1973; Malkin and Ivanchenko, 1983).

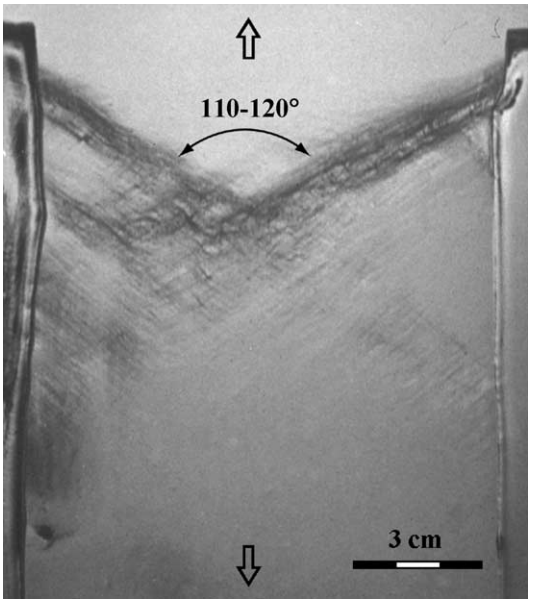

Fig. 7. Deformation pattern on the surface of the initially homogeneous wide plate (experimental photograph).

4. New experiments

In this section, we report results from four more experiments carried out using the same technique. The first experiment shows strain localization under ''flexible'' extensional boundary conditions considering the fact that the relative plate motion actually represents a rotation. The next three experiments are designed to gain insights into the strain localization pattern within the heterogeneous lithosphere model containing weak and strong zones.

4.1. Experiment 1

It differs from the experiment shown in Fig. 7 only by the boundary conditions illustrated in Fig. 8a. With this set up, we obtained a single linear propagating rift oriented at the same angle to the tension axis as in the previous experiments (Fig. 8b, compare with Fig. 3), while in Fig. 7, a double rift junction has been formed within the same model. Further investigations are needed to define whether this difference is due to the rotational/non rotational extension or simply

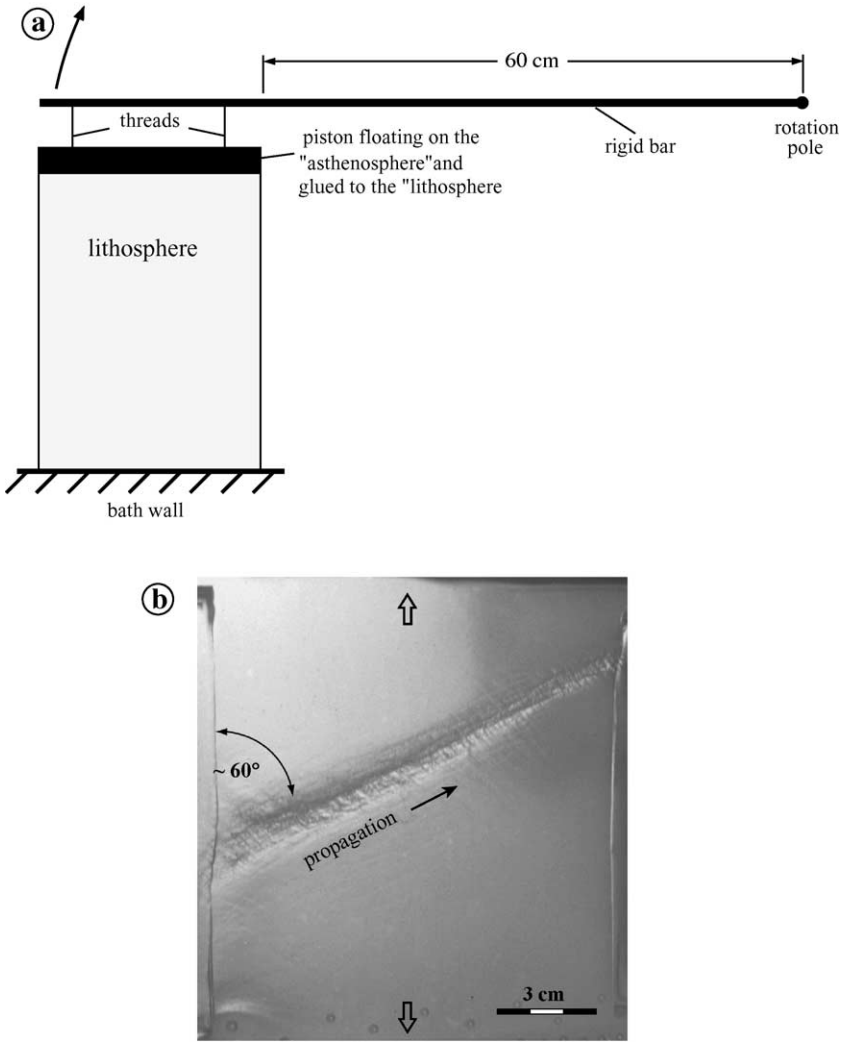

Fig. 8. Set up (a) and result (b) of the experiment with ''flexible'' boundary conditions (see text for more explanations).

because the boundary conditions in Experiment 1 (Fig. 8) are "flexible": The piston and the "lithosphere" glued to it are allowed to move in the direction perpendicular to the tension axis compatible with the strike–slip displacement along a single "rift". In Fig. 7, such a motion of the piston is "inhibited", and a stain localization within a wide plate should occur along two zones symmetrical with respect to the tension axis.

4.2. Experiment 2

The surface of the initially homogeneous lithospheric model was locally heated in the elongated zone shown in Fig. 9a. This caused the bulk plate strength in this zone to reduce by 20–30%. At the beginning of tension, the whole plate undergoes a stretching, which is the most intense (localized) within the "hot" zone. Simultaneously, two slip-line families appear within two fan-like areas at both sides of this zone (Fig. 9a and b) followed by the formation of four strain localization zones AB, BK, CD and CE (Fig. 9c). Two of them (BK and CD) evolve much slowly than the others and then die out, with deformation continuing only along the "rift system" ABCE (Fig. 9c).

4.3. Experiment 3

The thickness H of the continuous plate in the shaded area (Fig. 10) is ca. 20%, and the yield limit τ_s about 15% higher than in the rest of the lithosphere model where $\tau_s = 9.5$ Pa, and $H = 1.5 \times 10^{-2}$ m. In this model, the deformation occurs only within the thin and weak part of the plate. It starts first near the rigid "lithospheric" promontory. Then two families of slip-lines develop in the two fan-shape side areas and the deformation localizes along four zones (Fig. 10), in a way similar to the previous experiment.

4.4. Experiment 4

This experiment is designed to simulate the situation in the Baikal rift system (see discussion below)

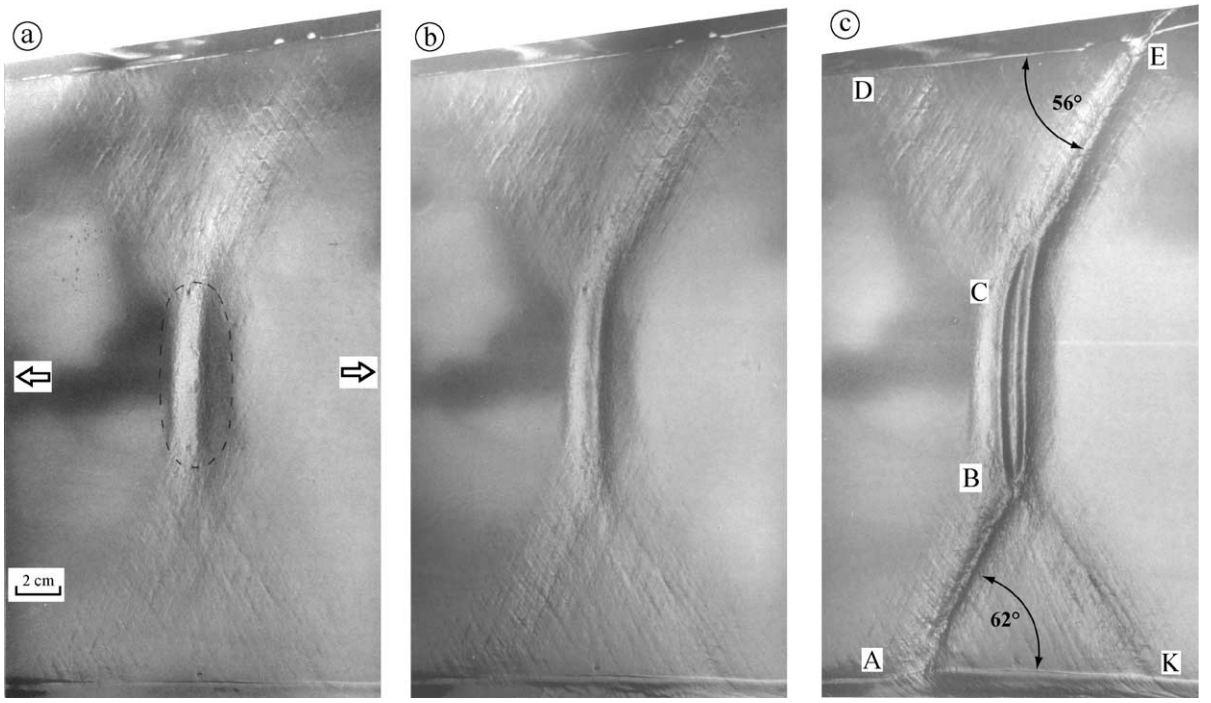

Fig. 9. Stretching of the model with elongated weak zone (contoured by the dashed line in (a)). Photographs are taken obliquely to the model surface; in reality opposite limits of the model are parallel.

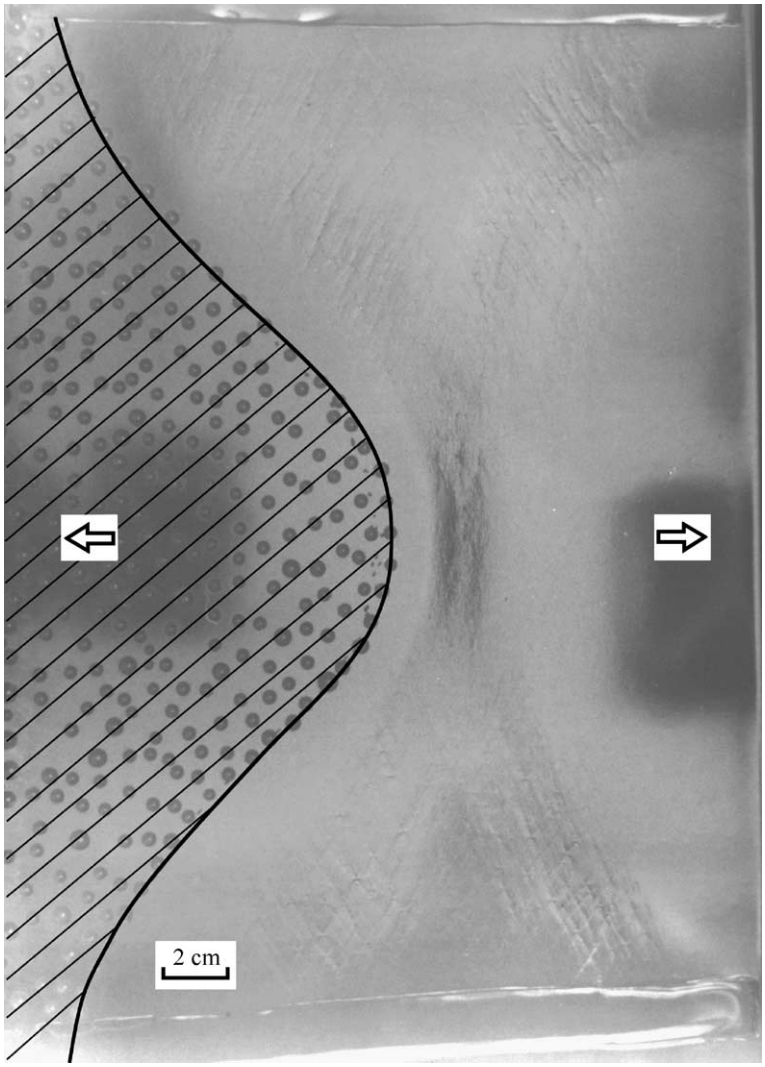

Fig. 10. Surface deformation pattern of the model consisting of two parts with strong and thick (dashed area) and weak and thin "lithospheres". The strain localization starts near the promontory of the strong lithosphere.

and combines the effects modelled in the two previous experiments (Experiments 2 and 3). Here the thick and rigid (cratonic) part of the lithospheric model has a sigmoid contour that mimics the shape of the Siberian (Archean) craton from the Angara to the North Lake Baikal regions (Fig. 12; see Sengör et al., 1993; Melnikov et al., 1994, and references therein). In addition, a small area at the contact between the two lithospheres (within a dashed line in Fig. 11a) is heated before extension as in Experiment 2 (Fig. 9) to produce a zone of weakness that may simulate either the hot spot or the fault zone. Extension in the direction indicated in Fig. 11a yields the following result: The strain first localizes in the weak orthogonal to the tension direction zone, resulting in the formation of a narrow deep valley. This is followed by shear/extensional strain localization along three wide (diffuse) oblique zones AB, BK and CE (see details in Fig. 11b). Zone BK evolves slower, with deformation mainly localizing along another conjugated branch AB. Deformation along BK ceases definitively after the complete failure of the litho-

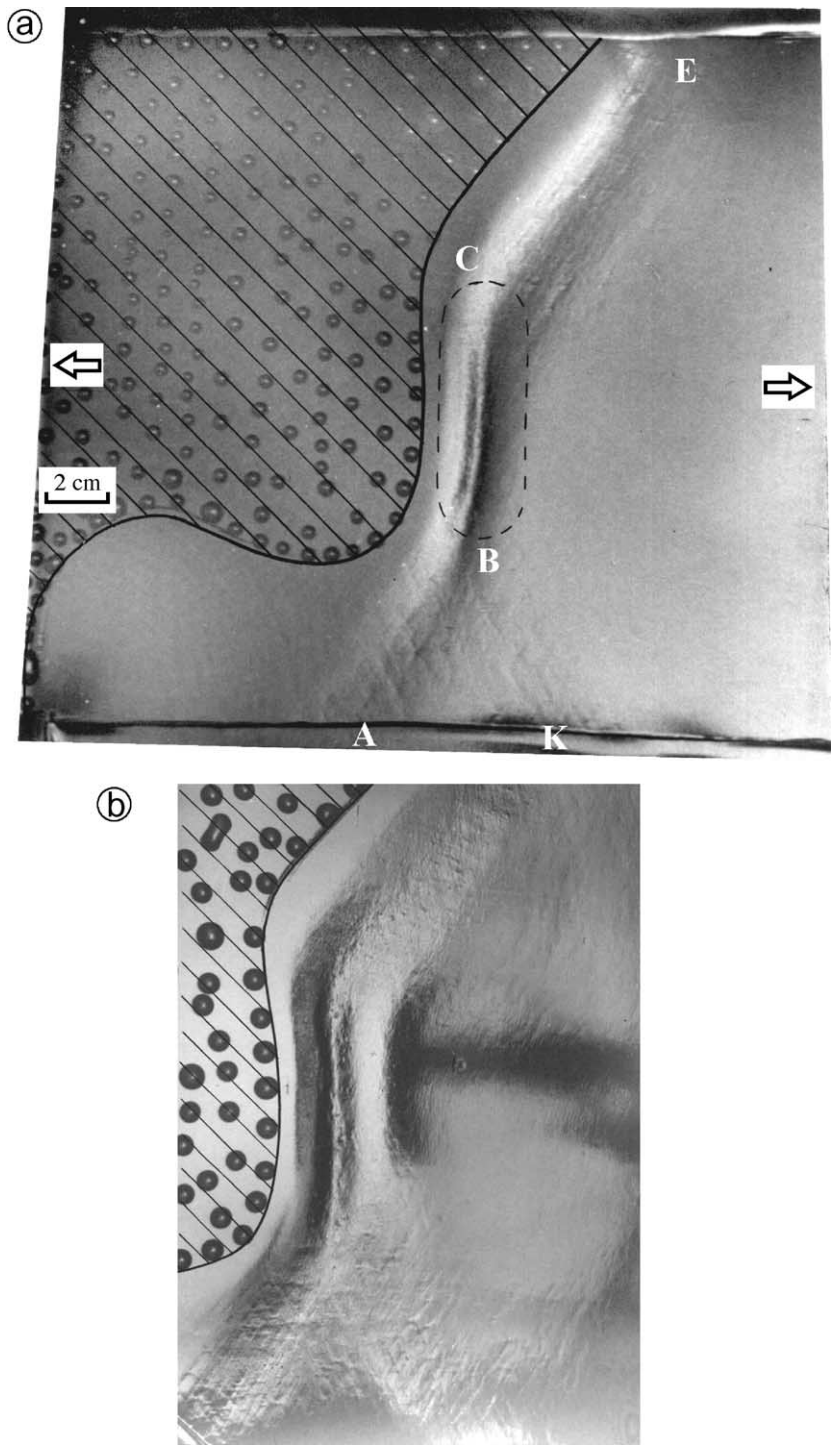

Fig. 11. Oblique top view of the deformed model with a strong lithosphere part (dashed) and a local weak zone, contoured by the dashed line. (a) Whole surface view; (b) close view of the deformation zone.

sphere (transition to spreading), which occurs along system ABCE (Fig. 11a). The result of this experiment is similar to Experiment 2 (Fig. 9), except that the oblique branch CD obtained in Experiment 2 does not form in Fig. 11 due to the presence at this place of a strong "cratonic" lithosphere.

We have conducted similar experiments but without preliminary weakening of the model near the cratonic promontory in the central part of the model (along the segment CB; Fig. 11a) but did not obtain a clear result. A strain localisation started in this case near the Points E and A and evolved to connect these points along a wide zone of strain localisation. The deformation along this zone then has been stopped as the localisation occurred along the piston (boundary effect) which is to the right in Fig. 11. These experiments show that the strain localisation does not follow the craton boundary (does not go through the segment CB). In other words, "rifting" along the segment CB is impossible if the lithosphere is not weakened at this place.

5. Discussion of the experimental results

The described experiments correspond to a passive rifting mechanism. Model rifts represent zones of strain localization with the following properties: First, these zones are generally not orthogonal to the tension axis (or stretching direction) and are oriented at an angle of 55°–60° to it in the homogeneous model. This angle persists even when the rate of divergence between the opposite plate boundaries is not constant and varies laterally proportionally to the distance to the pole of relative rotation of these boundaries. In this case, the zone of strain localization propagates rapidly approaching the pole of rotation. Such a propagation is documented in many old and active rifts (Courtillot, 1982; Bossworth, 1985; McKenzie, 1986). The obtained characteristic angles of 110°–120° (and not ~90° as in the case of plastic deformation/failure under plane-strain conditions) between the two families of the Luders lines and the zones of deformation localization follow from the theory of plasticity. The plastic lithospheric plate in our experiments deform under the plane-stress conditions and can be described by an hyperbolic system of equilibrium equations that has two conjugated families of characteristics (Kachanov, 1971). It can be shown that for the boundary conditions applied in the experiments (uniform uniaxial tension), the families are linear, intersected at an angle 2ψ of about 110° (more exactly 109.46°) and make an angle ψ with the tension direction (Kachanov, 1971): These angles are very close to those observed in the experiments.

The characteristic lines have interesting properties: In particular, the normal deformation along them is zero. They can represent also the lines of the velocity discontinuity and the localization deformation (as is observed in our experiments). The deformation localization (plastic failure) along these (characteristic) directions corresponds also to a minimal "driving" tensional stress σ_1 (Nadai, 1950). Indeed, in the case of the discontinuous solution (necking formation), this stress can be related to ψ as follows (Kachanov, 1971):

$$\sigma_1 = \tau_s \frac{1 - 3\cos 2\psi}{\sqrt{1 + 3\cos^2 2\psi}} \quad (2)$$

where τ_s is the shear yield limit. σ_1 takes a minimal value equal to $\sqrt{3}\tau_s$ when $d\sigma_1/d\psi = 0$, i.e., at $\psi = 54.73° \approx 55°$. For $\psi = 90°$ (necking orthogonal to the tension axis), $\sigma_1 = 2\tau_s$. As the work on a plastic deformation of the plate is proportional to $\sigma_1 \times \Delta l$ (Δl is the amount of extension), the angle $\psi \approx 55°$ has an energetic meaning and corresponds to a minimal energy dissipation during plastic strain localization.

Plate failure in the direction perpendicular to tension can thus occur only if the lithosphere is weakened enough (by $>100\% \times (2\tau_s - \sqrt{3}\tau_s)/\sqrt{3}\tau_s = 15.5\%$) along this direction, as it was the case in Experiments 2 and 4 (Figs. 9 and 11). In the experiments with a vertical cut (Fig. 5), the lithospheric material was not weakened; we just created an interface (cut) between the two rigid plate parts (blocks). Separation of these blocks under tension is impossible because of the hydrostatic suction between the blocks (Malkin and Shemenda, 1991). The separation in this situation can occur along an inclined surface that must be formed. In other words, the lithosphere should be broken again as it has occurred in the experiment shown in Fig. 5. However, before reaching the failure condition for $\psi \approx 90°$ ($\sigma_1 = 2\tau_s$, cut perpendicular to the tension axis), the deformation

localization (failure) will start at a lower stress of $\sqrt{3}\tau_s$ but along a direction at $\psi \approx 55°$. This is exactly what has been observed in the described experiments. Failure at $\psi \approx 90°$ has been obtained only when we created a fault zone with many cuts (or an inclined cut). Such a zone can be considered as a zone with reduced effective strength of the lithospheric material and behaves similarly to the ''hot spots'' where material weakening was achieved by heating. The important conclusion following from the above analysis and conducted experiments is that the lithosphere does not ''feel'' the presence of a weak zone oriented perpendicular to the tension axis if the effective strength reduction in this zone is less than $\sim 15\%$.

In plane-stress approximation, the vertical nonhydrostatic stress is zero and the two other principal stresses σ_1 and σ_2 ($\sigma_1 > \sigma_2$) are horizontal. One stress in the lithosphere (in our case, the extensional stress σ_1) is always dominant, but in nature, the other one, σ_2, is not necessarily zero. Let us see whether angle ψ is highly sensitive to the σ_2 value. This angle is related to the principal stresses by:

$$\cos(2\psi) = -\frac{\sigma_1 + \sigma_2}{3(\sigma_1 - \sigma_2)} \tag{3}$$

where stresses in a plastic state cannot be arbitrary and must satisfy the Mises' criterion (Kachanov, 1971):

$$\sigma_1^2 - \sigma_1\sigma_2 + \sigma_2^2 = 3\tau_s^2 \tag{4}$$

From (3) and (4), it follows that if σ_2 is also tensional, the ψ value increases with reducing σ_1/σ_2 ratio but not strongly. For example, for $\sigma_1/\sigma_2 = \infty$ ($\sigma_2 = 0$), $\psi = 54{,}73°$ as was obtained previously, while for $\sigma_1/\sigma_2 = 3.7$, it increases only to 62.6°. When σ_2 is compressional (negative), ψ decreases with $|\sigma_1/\sigma_2|$ reduction such that for $\sigma_1/\sigma_2 = -4.4$, $\psi = 51°$. These estimates thus show that 50°–60° represents a reasonable range for the ψ value that one might expect to find in natural rift systems where σ_2 is unlikely to be equal to zero.

The necking width in the experiments is comparable to the plate thickness, i.e., several tens of kilometres (mechanical lithosphere thickness) in nature, which corresponds to the average observed rifts width (Allemand and Brun, 1991; Ruppel, 1995; Olsen, 1995). On the other hand, numerous experiments (e.g., Shemenda and Grokholsky, 1991) show that the failure of a brittle plate subjected to the same boundary conditions occurs along very narrow vertical or inclined brittle cracks forming perpendicular to the tension axis. The fact that most rifts do not generally strike orthogonal to the stretching direction (see, e.g., Bonini et al., 1997; Malkin and Ivanchenko, 1983, and references therein) suggests that the bulk behaviour of the lithosphere corresponds to a plastic model rather than to a brittle one. A similar conclusion follows from rock mechanics experiments showing that the thickest and strongest part of the lithosphere has plastic properties (Kohlstedt et al., 1995). The neck (rift) junctions at an angle of 110°–120° obtained in the experiments and often observed in nature (Burke and Dewey, 1973; Malkin and Ivanchenko, 1983) yield additional strength to this conclusion.

The experiments show that faulting in the upper lithospheric layers does not influence considerably the large (lithospheric)-scale configuration of the rift zones. As shown in Fig. 5, such a faulting can affect the lithosphere deformation in cross-section, making it asymmetrical (if the downward propagation of these faults is not limited in nature by the weak, ductile lower crust). In any case, the superficial brittle faulting seems to not affect the rift geometry in a map view. On the other hand, the lithospheric-scale faults (fault zones) as well as other lithospheric-scale heterogeneities (weak and strong zones) have a major impact on the rifting process as shown by the presented experiments (see also Tron and Brun, 1991; Bonini et al., 1997). The initiation of strain localization can occur not only in a weak zone but also near the promontory of a rigid zone as seen in Fig. 10. It is interesting to note that the cratonic stiff promontories cause strain to localize within the adjacent weaker lithosphere not only under extension (as in Fig. 10), but also under compressional and shear stresses, as shown by 3-D modelling of intraplate deformation south of India (Shemenda, 1994) or in Brazil (Tommasi et al., 1995). In the last experiment (Fig. 11), we introduced into the model both weak (hot) and strong (cold) zones in order to simulate the situation in the Baikal rift system that we consider in detail below.

6. Baikal rift system

6.1. Geometry and kinematics

The Baikal rift system is located close to the S-shaped Paleozoic suture that separates the Siberian craton from the so-called Sayan–Baikal folded belt (Fig. 12; Logatchev and Zorin, 1992; Sengör et al., 1993; Melnikov et al., 1994; Zorin, 1999). The present-day stress field is characterized by a roughly constant (over the whole area) orientation of the extensional axis N(120°–135°)E (Fig. 12a; Petit et al., 1996; San'kov et al., 2000). Fault scarps (San'kov et al., 2000) and GPS measurements (Calais et al., 1998) yield horizontal extension rates of a few millimetres per year for at least Plio-Quaternary times. The rift can be schematically divided into three major segments or branches (Fig. 12; Logatchev and Florensov, 1978; Tapponnier and Molnar, 1979).

6.1.1. The western rift branch

The western rift branch (AB, Fig. 12) is a ~ N75E-trending, 400-km-long and up to 150-km-wide zone of deformation that includes the active NS-striking basins of Busingol, Darkhat, Hövsgöl and the EW-trending Tunka basin. This zone is dominated by wrench faulting with E–W and N–S average faults orientations (San'kov et al., 1997; Larroque et al., 2001). Focal mechanism solutions show that both normal and reverse faulting occurring on NW–SE and/or NE–SW planes are present as well (Fig. 12b; Petit et al., 1996). About 200 km south of this branch, the large Bolnai–Tsetserleg fault system (Fig. 12a), with similar trends (W–E and NE–SW) and kinematics, was the place of one of the largest intracontinental earthquake sequence ever felt ($M=8.0$, Tsetserleg, and $M=8.4$, Bolnai, 1905 earthquakes; see, e.g., Baljinnyam et al., 1993; Schlupp, 1996). The contact of the western rift branch with the craton is located near the main Sayan fault zone (Fig. 12a). The angle between this branch and the mean regional direction of extension is ca. 50° (see inset in Fig. 12b).

6.1.2. The central rift branch

The central rift branch (BC, Fig. 12) runs in the N40E° mean direction over 650 km and coincides with Lake Baikal. It is relatively narrow (~ 80 km) and is settled just close and parallel to the marginal suture between the craton and the Sayan–Baikal belt. At the surface, the rift opening is controlled by the Primorsky fault zone, an old inherited structure which probably merges with the suture zone at depth (Logatchev and Florensov, 1978; Delvaux et al., 1995). Since at least 4 Ma extension here is nearly orthogonal to the rift axis and generates normal faulting (Sherman, 1992; Petit et al., 1996; Delvaux et al., 1997).

6.1.3. The eastern rift branch

The eastern rift branch (CE, Fig. 12), also called the North Baikal Rift, has ~ N70° strike, extends over ~ 800 km and is up to 300 km wide. This branch is entirely settled within the Sayan–Baikal belt. The extensional features (Fig. 12a) as well as the tensional seismicity vanish toward the Aldan shield promontory (Melnikov et al., 1994). The dominant fault orientation N60°E (Sherman and Gladkov, 1999; San'kov et al., 2000) is in a good agreement with the statistically representative strike of the nodal planes. This branch makes an angle of about 50° with the mean regional extension direction.

6.2. Deep rift structure and time–space evolution of rifting

Deep structure of the rift has been long a subject of much debate that largely concentrated around passive versus active rift origin (e.g., Zorin, 1981; Logatchev et al., 1983; Kiselev and Popov, 1992; Gao et al., 1994;

Fig. 12. Geodynamic setting (a) and seismicity (321 fault plane earthquake solutions) (b) of the Baikal rift. Thick dotted line is the limit between the stiff cratons and the softer Sayan–Baikal belt. Thick dashed lines show the mean directions of the rift branches deduced from the active fault traces and seismicity. Sketch in the inset in (b) summarizes the main orientations of the rift branches (corresponding to the thick dashed lines in (a) and (b)), GPS vectors (thin arrows), and mean fault strikes and stress directions from tectonic and seismological studies (thin lines and large black arrows, respectively). Main faults are from Tapponnier and Molnar (1979), Déverchère et al. (1993) and Bayasgalan et al. (1999). Focal mechanisms are from Petit et al. (1996), Schlupp (1996) and Larroque et al. (2001). GPS strikes are from Calais et al. (1998, 2000) and Calais and Amarjargal (2000). Abbreviations of basin names are as follows: B, Busingol, D, Darkhat, H, Hövsgöl, T, Tunka. The names of main faults (F) are shown in (a) and the years of $M>7$ events since 1900 are indicated in (b). Lambert conic projection is used (crosses show N–S and E–W directions) in maps (a) and (b), whereas plane projection (constant direction) is used in the inset of (b).

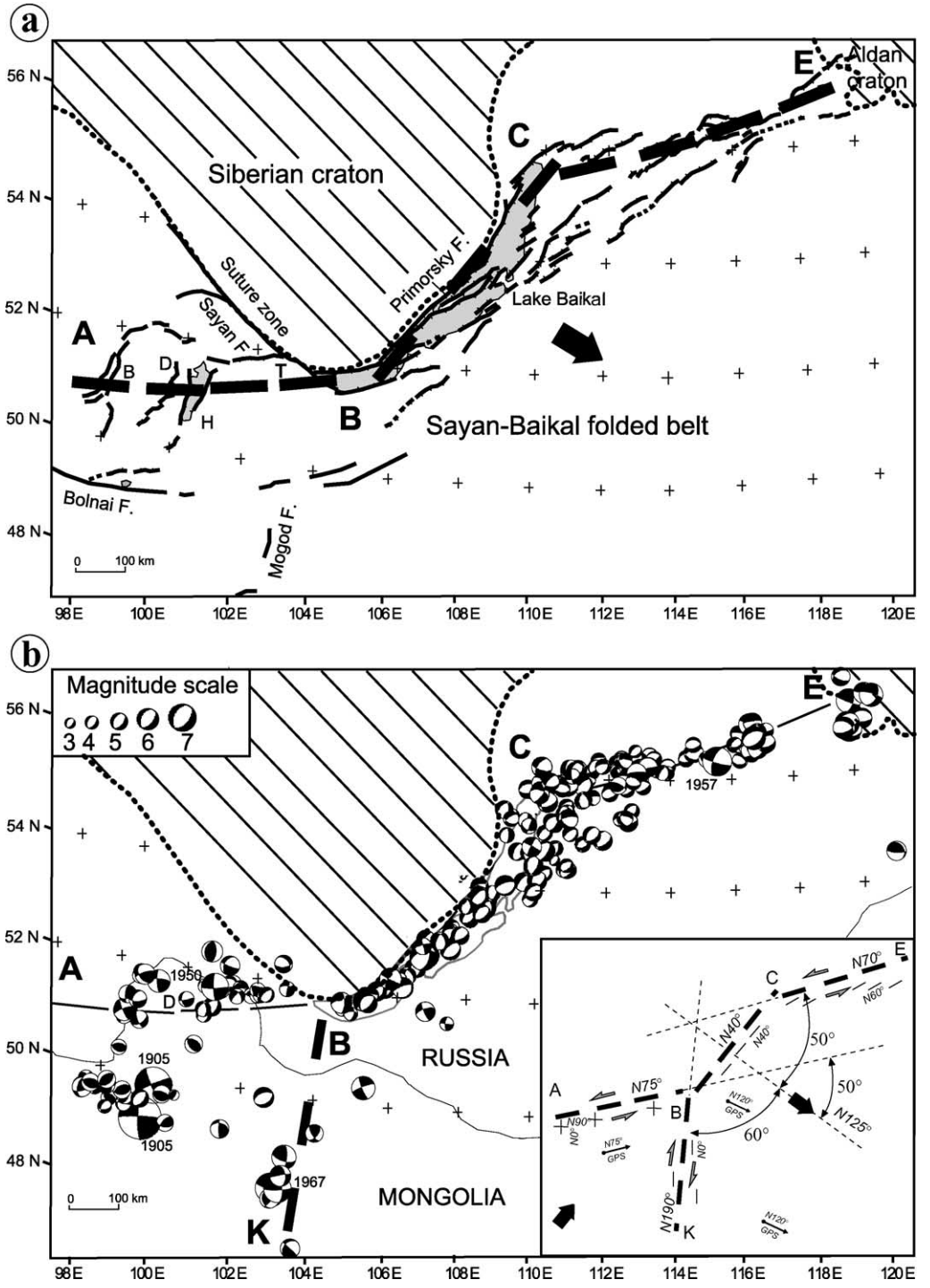
a
Aldan craton
E
C
Siberian craton
Primorsky F.
Suture zone
Sayan F.
Lake Baikal
A
B
D
T
H
B
Sayan-Baikal folded belt
Bolnai F.
Mogod F.
0 100 km
56 N
54 N
52 N
50 N
48 N
98E
100E
102E
104E
106E
108E
110E
112E
114E
116E
118E
120E
b
Magnitude scale
3 4 5 6 7
1957
1950
1905
1905
1967
RUSSIA
MONGOLIA
K
N70°
N60°
N40°
N75°
N90°
N125°
50°
50°
60°
N190°
GPS

Popov, 1990; Lysak, 1995; Petit et al., 1998). From numerous recent tomographic studies at various scales (Petit et al., 1998; Ritzwoller and Levshin, 1998; Curtis et al., 1998; ten Brink and Taylor, 2002; Villaseñor et al., 2001), it appears that there is no large thermal "disturbance" of the asthenosphere below the lake that would advocate either for a large-scale mantle upwelling or lithospheric thinning. On the other hand, it became clear that the Paleozoic suture zone between the Siberian craton and Sayan–Baikal belt is a major factor controlling the structuring and lithospheric-scale asymmetry of the rift (Lesne et al., 2000). According to these authors, the rifting resulted from passive simple shear extension localized on this inherited lithospheric discontinuity, although no low-angle detachment fault zone at depth has been directly evidenced. Such a fault has been suggested based on experimental seismology (Puzyrev et al., 1978; Popov, 1990; Logatchev and Zorin, 1992), structural geology data (Houdry, 1994; San'kov et al., 2000) and off-rift volcanic activity (Kazmin, 1991) started during Paleogene (Rasskazov, 1994), i.e., approximately at the onset of rifting.

It is believed that the evolution of the Baikal rift comprises two phases corresponding to "slow" and "fast" rifting, which have approximately occurred at 30 to 3 Ma and 3 Ma to present, respectively (Logatchev and Zorin, 1987, 1992; Delvaux et al., 1997; San'kov et al., 1997; Kuzmin et al., 2000, and references therein), although this two-step evolution is still debated (e.g., ten Brink and Taylor, 2002). The orientation of the stress field remained more or less constant since $\sim 10-7$ Ma (San'kov et al., 1997, 2000). Finally, although the spatial and time evolution (propagation in particular) of the rift are not reliably constrained (San'kov et al., 2000; Kuzmin et al., 2000), most authors agree that the rifting was initiated in the southern and central Lake Baikal and then propagated to its present limits (Logatchev and Zorin, 1992; San'kov et al., 1997, 2000).

6.3. Comparison with the modelling results and discussion

6.3.1. Overall configuration of the rift system

The first-order three-branch structure of the Baikal rift system has been reproduced in various experimental configurations. For example, in Experiment 2 (Fig. 9), such a structure was obtained in a homogeneous lithospheric model containing only one linear weak zone (fault zone, for example). The deformation localization (necking), hence, formation of the valley (basin), first occurs in this central orthogonal to extension weak zone. Then four other oblique and wider (diffused) zones of deformation appear. Two of them BK and CD develop slowly and are entirely abandoned after the complete failure of the lithosphere model along a three-branch system ABCE (Fig. 9c). The Baikal system also contains one central "normal" and narrow branch where rifting was initiated first and the two oblique wide branches (Fig. 12). The eastern branch CE in Experiment 2 (Fig. 9) is oriented to the central segment BC (corresponding to Lake Baikal) at approximately the same angle as in nature ($\sim 50^\circ$ to the extension direction, see inset in Fig. 12b). The orientation of the western branch AB is also close in the experiment and nature. Thus, it appears that the sharp rheological contrast between the Siberian craton and the Sayan–Baikal belt is not necessary to generate the Baikal rift system: The weak (suture) zone that certainly exists between these two geologically distinct units is sufficient. If this were the case, we should see in nature the traces of the two aborted diffuse oblique branches KB and CD obtained in the experiment (Fig. 9). There is, however, no indication of the past (since the rifting onset) or present activity NW of Lake Baikal in the area corresponding to the northern branch CD in Fig. 9. This zone thus did not form in nature. The simplest way of prohibiting formation of this zone in experiments is to increase the effective lithospheric strength in this area. It has been done in Experiment 4 (Fig. 11) where the northern branch has not been formed. The rheological contrast between the craton and the Sayan–Baikal belt is thus necessary to better approach the actual rift structure. On the other hand, the southern diffuse oblique branch BK occurs always in the experiments with or without the rheological contrast, since this branch is entirely located within the weak lithosphere. Does this zone (the "fourth rift branch") exist in nature?

6.3.2. The fourth rift branch?

A simple look at the seismicity map (Fig. 12b) is enough to reveal a significant activity in the area corresponding to the fourth branch BK predicted by the experiment. A diffuse plate boundary in this area has been already proposed from kinematic constraints

(Zonenshain and Savostin, 1981; Lesne et al., 1998) and is documented by some tectonic observations (Baljinnyam et al., 1993; Bayasgalan et al., 1999). The shear displacement along this boundary following from the experiment is consistent with the preliminary GPS data (Fig. 12b, inset; Calais et al., 1998, 2000; Calais and Amarjargal, 2000) and with the strike of the nodal planes from focal mechanisms (Fig. 12b): Both attest for the right-lateral shear in the area corresponding to the hypothetic branch BK. The large ($M=7.1$) Mogod earthquake in 1967, for instance, was associated with a displacement along an ~20-km-long, right-lateral, N–S strike–slip fault (Fig. 12; Baljinnyam et al., 1993; Bayasgalan et al., 1999). There are also a few active fault segments striking from W–E to N60°E (Fig. 12a) that may correspond to the second family of fractures (slip-lines) obtained in the experiments (see Fig. 13). It thus seems that the fourth branch BK, although weakly expressed, does exist, is presently active and is oriented to the regional extension direction at an angle of 50°–60° (Fig. 12b, inset) consistent with the modelling results. Notice that the overall configuration of the four-branch Baikal rift system on the inset in Fig. 12 is remarkably similar to the experiment model in Fig. 11 (see also Fig. 13).

There are evidences that the fourth branch was active in the past. Close to (and just west of) line BK in Fig. 12b various types of "anomalies" have been documented: the elevated topography (Hangai dome; Windley and Allen, 1993; Cunningham, 1998), low P- and S-wave velocities at 100–400 km depth (Curtis et al., 1998; Petit et al., 1998; Villaseñor et al., 2001) and moderate thermal disturbance at the uppermost mantle evidenced by xenoliths (Ionov et al., 1998). Most importantly, the area near line BK is characterized by concentration of Cenozoic volcanism (Kiselev, 1987) that first occurred near the Tunka basin during Paleogene and was active mostly from Oligocene until

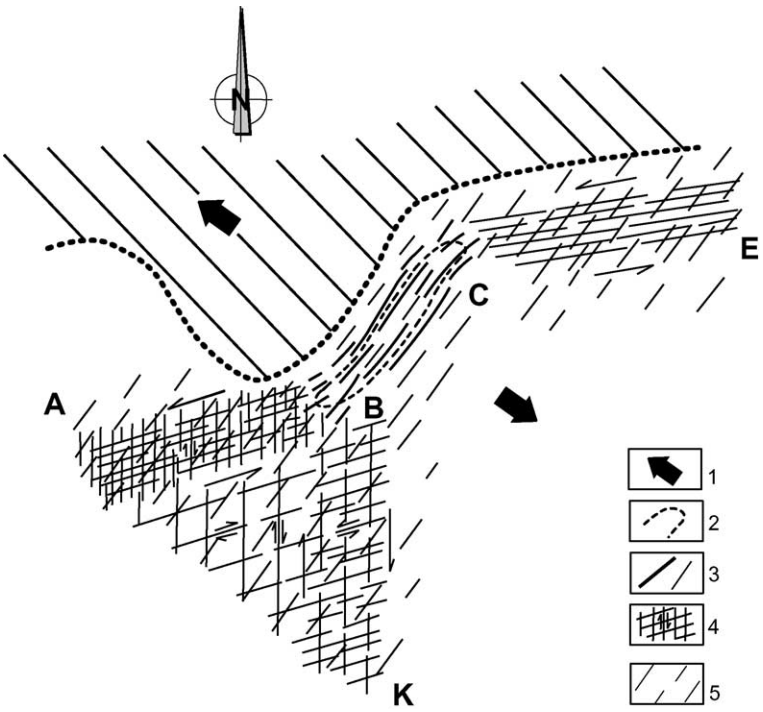

Fig. 13. First-order surface deformation pattern in the Baikal area at the onset of the rifting (based on the Experiment 4 in Fig. 11). (1) Regional tension vector; (2) contour of the deepest part of the depression formed in the experiment (corresponds to Lake Baikal); (3) lithospheric-scale normal faults in the lake area; (4) Luders lines in the "plastic core" of the lithosphere that may propagate to the surface trough the brittle part of the lithosphere; (5) normal faults and cracks that should form in the upper brittle crustal layer perpendicular to the tension direction in the whole area.

Quaternary (Rasskazov, 1994). This volcanic "belt" extends over ~1000 km from the southern Lake Baikal to the south, crossing central Mongolia (Kiselev, 1987). Thus, the southern branch BK was active since initial rifting but remains underdeveloped and does not have clear tectonic manifestation, which means that the displacement along this branch was much smaller than along the others. Was this displacement continuous since the rifting onset or interrupted and recently reactivated? The two options seem possible. In the conducted experiments, the branch BK dies after a few millimetres of stretching (Δl) that corresponds to a few tens of kilometres in nature (Δl depends largely upon the strain weakening of the model material and also upon the model width/length ratio and boundary conditions (their tightness)). Since the Baikal rifting is slow and the stretching amount is small ($\Delta l < 10$ km, San'kov et al., 2000), this process can be still at the stage when branch BK keeps dying activity. Another possibility is that this branch has died and recently has been reactivating, owing to the compressional front arriving from the Himalayas due to the India–Eurasia collision. Indeed, the collision has started 50–60 Ma ago (Qayyum et al., 1997; DeSigoyer et al., 2000) and was continuously propagating toward the north. It reached the Tarim basin around 20 Ma (Mattauer et al., 1999), northern Mongolia ca. 8 Ma (Baljinnyam et al., 1993; Schlupp, 1996; Cunningham et al., 1996; Cunningham, 1998) and affected the western branch AB of the Baikal system only in Quaternary (Larroque et al., 2001). Therefore, it seems that the Baikal rifting, initiated in Paleogene (Oligocene) times (Logatchev and Zorin, 1992), was not generated by the India–Asia collision and has been developing since the beginning under ~SE extension whose origin, however, remains unclear. The compressional front recently arrived from the south (Larroque et al., 2001) may have suppressed extension along the western rift branch AB and, as a consequence, it may have caused the reactivation of the southern branch BK accommodating a left-lateral shear and extension (see inset in Fig. 12b).

7. Conclusion

The rheological structure of the continental lithosphere is poorly known and, certainly, is complex. Traditionally, the lithosphere is represented by a three (or more)-layer model with a strong upper crust and lithospheric mantle, and a weak lower crust. Among other factors, the rheological structure is very sensitive to the composition of the crust which by its nature is laterally and vertically very heterogeneous. Therefore, its mechanical structure is rather spotty than layered: In some zones, a weak lower crust exists and in others not (Ranalli, 2000). Numerous data argue, for example, that in the Baikal region, the whole crust is relatively strong (Déverchère et al., 2001, and references therein). Ideally, we had to create such a spotty lithosphere model consisting of one- and three (or more)-layer segments. In this paper, however, we limited ourselves to a simple, first-order approximation, using a one-layer lithosphere model, but varying laterally its effective strength. This variation can correspond to the variation of the plate thickness and geotherm, but also to the variation of the weak crustal layers thickness (these layers reduce the effective lithosphere strength). It is clear that such a model cannot reproduce details of lithosphere deformation in cross-section, but it seems that it can satisfactorily represent large-scale deformation of the lithosphere in plane. On this scale, the lithosphere is in a plane-stress state and its behaviour is controlled by the integral (over the thickness) properties, with the details of vertical lithosphere structure being less important. The lithospheric deformation in cross-section (necking) largely depends, as mentioned, on its rheological stratification, but it also depends on the configuration of a rift zone in map view. Our modelling shows that this configuration is controlled by the lateral mechanical (e.g., rheological) heterogeneities. Zones of strain localization avoid strong (cold) lithospheric areas and cross weak areas such as hot spots and lithospheric-scale fault zones. This is an intuitively understandable conclusion. What is less obvious is that the promontories of a strong (cratonic) lithosphere have been proven to "attract" zones of strain localization that can be initiated in their vicinity. The configuration (hence, dynamics) of a rift zone is therefore defined by the spatial distribution of strong and weak lithospheric areas. The strain localization zones thus represent essentially 3-D structures even within a homogeneous lithosphere subjected to a uniaxial tension, since they normally form obliquely to the tension direction. This obliquity is due to the

plastic bulk properties of the lithosphere deforming under plane-stress conditions. In a homogeneous plate, zones of strain localization are oriented at $\pm 50°-60°$ to the extension axis even when the divergent displacement of the plates is not translational but rotational. In the latter case, the strain localization zone is propagating in a direction of $50°-60°$ with respect to the tension axis. In many experimental configurations, strain localization occurs along double ''rifts'' conjugated at an angle of $2 \times (50°-60°) \approx 110°$ frequently observed in nature. The configuration of a particular rift system should be defined thus by the interplay of all these factors: presence and geometry of weak and strong zones as well as the tendency of strain to localize in a direction oblique to the tension axis.

The modelling of the Baikal rift system has confirmed the major role of a weak zone (suture) known in the area of Lake Baikal and of a sharp rheological contrast between the Siberian craton and the Sayan–Baikal warmer lithosphere in structuring this system. By introducing these heterogeneities into the experimental model, we were able to obtain a well-known three-branch structure of the Baikal rift system with one orthogonal (central) narrow branch (corresponding to Lake Baikal) and two oblique branches. The modelling predicts also the formation of a fourth southern ~ NS-trending branch (oblique strain localization zone). There are field data corroborating the existence of this poorly expressed feature. Orientation of all four branches with respect to each other and to the regional tension direction is in a good correspondence with the experimental model (compare inset in Fig. 12b with Fig. 11 or Fig. 13).

Acknowledgements

We thank J.-P. Brun and P. van der Beek for helpful reviews.

References

Allemand, P., Brun, J.P., 1991. Width of continental rifts and rheological layering of the lithosphere. Tectonophysics 188, 63–69.

Allemand, P., Brun, J.P., Davy, Ph., van der Driessche, J., 1989. Symétrie et asymétrie des rifts et mécanismes d'amincissement de la lithosphere. Bull. Soc. Geol. France 8 (3), 445–451.

Artyushkov, E.V., 1981. Mechanisms of continental riftogenesis. Tectonophysics 73, 9–14.

Baljinnyam, I., Bayasgalan, A., Borisov, B.A., Cisternas, A., Dem'yanovich, M.G., Ganbaatar, L., Kochetkov, V.M., Kurushin, R.A., Molnar, P., Philip, H., Vashchilov, Y.Y., 1993. Ruptures of major earthquakes and active deformation in Mongolia and its surroundings. Geol. Soc. Amer. Mem. 181, 62 pp.

Bayasgalan, A., Jackson, J., Ritz, J.F., Carretier, S., 1999. Field examples of strike–slip fault termination in Mongolia and their tectonic significance. Tectonics 18, 394–411.

Benes, V., Davy, P., 1996. Modes of continental lithospheric extension: experimental verification of strain localization processes. Tectonophysics 254, 69–87.

Bonini, M., Souriot, Th., Boccaletti, M., Brun, J.P., 1997. Successive orthogonal and oblique extension episodes in a rift zone: laboratory experiments with application to the Ethiopian rift. Tectonics 16 (2), 347–362.

Bossworth, W., 1985. Geometry of propagating continental rifts. Nature 316, 625–627.

Brun, J.P., Beslier, M.O., 1996. Mantle exhumation at passive margins. Earth Planet. Sci. Lett. 142, 161–173.

Buck, W.R., 1991. Modes of continental lithospheric extension. J. Geophys. Res. 96, 20161–20178.

Burke, K., Dewey, J.F., 1973. Plume generated triple junctions: key indications in applying plate tectonics to old rocks. J. Geol. 81, 406–433.

Burov, E., Poliakov, A., 2001. Erosion and rheology controls on synrift and postrift evolution: verifying old and new ideas using a fully coupled numerical model. J. Geophys. Res. 106, 16461–16481.

Calais, E., Amarjargal, S., 2000. New constraints on current deformation in Asia from continuous GPS measurements at Ulan Baatar, Mongolia. Geophys. Res. Lett. 27 (10), 1527–1530.

Calais, E., Lesne, O., Déverchère, J., Sankov, V.A., Lukhnev, A.V., Miroshnichenko, A.I., Levi, K.G., 1998. Crustal deformation in the Baikal rift from GPS measurements. Geophys. Res. Lett. 25 (21), 4003–4006.

Calais, E., Vergnolle, M., Lesne, O., Déverchère, J., Sankov, V.A., Lukhnev, A.V., Miroshnichenko, A.I., Bashkuev, Y., Zalutzky, V., Amarjargal, B., 2000. Crustal Deformation in Asia: New Constraints from GPS Measurements in the Mongolia–Baikal Area. Am. Geophys. Union, San Francisco (Abstract).

Courtillot, V., 1982. Propagating rifts and continental breakup. Tectonics 1, 239–250.

Cunningham, W.D., 1998. Lithospheric controls on late Cenozoic construction of the Mongolian Altai. Tectonics 17, 891–902.

Cunningham, W.D., Windley, B.F., Dorjnamjaa, D., Badamgarov, J., Saandar, M., 1996. Late Cenozoic transpression in southwestern Mongolia and the Gobi-Altaï Tien Shan connection. Earth Planet. Sci. Lett. 140, 67–81.

Curtis, A., Trampert, J., Snieder, R., Dost, B., 1998. Eurasian fundamental mode surface wave phase velocities and their relationship with tectonic structures. J. Geophys. Res. 103, 26919–26947.

Delvaux, D., Moeys, R., Stapel, G., Melnikov, A., Ermikov, V.,

1995. Paleostress reconstruction and geodynamics of the Baikal region, Central Asia: I. Paleozoic and Mesozoic pre-rift evolution. Tectonophysics 252, 61–101.

Delvaux, D., Moeys, R., Stapel, G., Petit, C., Levi, K.G., Miroshnichenko, A.I., Ruzhich, V.V., San'kov, V.A., 1997. Paleostress reconstructions and geodynamics of the Baikal region, Central Asia: Part II. Cenozoic rifting. Tectonophysics 282, 1–38.

DeSigoyer, J., Chavagnac, V., Blichert-Toft, J., Cosca, M., Guillot, S., Luais, B., Mascle, G., Villa, I., 2000. Dating the Indian continental subduction and collisional thickening in NW Himalayas: multichronometry of the Tso Morari eclogites. Geology 28, 487–490.

Déverchère, J., Houdry, F., Solonenko, N.V., Solonenko, A.V., Sankov, V.A., 1993. Seismicity, active faults and stress field of the North Muya region, Baikal rift: new insights on the rheology of extended continental lithosphere. J. Geophys. Res. 98, 19895–19912.

Déverchère, J., Petit, C., Gileva, N., Radziminovitch, N.A., Melnikova, V.I., San'kov, V.A., 2001. Depth distribution of earthquakes in the Baikal rift system and its implications for the rheology of the lithosphere. Geophys. J. Int. 146, 714–730.

Dunbar, J.A., Sawyer, D.S., 1989. How preexisting weaknesses control the style of continental breakup. J. Geophys. Res. 94, 7278–7292.

Faugères, E., Brun, J.P., Van den Driessche, J., 1986. Bassins asymétriques en extension pure et en décrochement: modèles expérimentaux. Bull. Soc. Nat. Elf-Aquitaine Prod. 10, 13–21.

Forsyth, D.W., Uyeda, S., 1975. On the relative importance of the driving forces of plate motion. Geophys. J. R. Astron. Soc. 43, 163–200.

Gao, S., Davis, P.M., Liu, H., Slack, P.D., Zorin, Y.A., Mordvinova, V.V., Kozhevnikov, V.M., Logatchev, N.A., 1994. Seismic anisotropy and mantle flow beneath the Baikal rift zone. Nature 371, 149–151.

Hassani, R., Chéry, J., 1996. Anelasticity explains topography associated with Basin and Range normal faulting. Geology 24, 1095–1098.

Hopper, J.R., Buck, W.R., 1996. The effect of lower crustal flow on continental extension and passive margin formation. J. Geophys. Res. 101, 20175–20194.

Hopper, J.R., Buck, W.R., 1998. Styles of extensional decoupling. Geology 26 (8), 699–702.

Houdry, F., 1994. Mécanismes de l'extension continentale dans le rift nord-Baïkal, Sibérie: contraintes des données d'imagerie SPOT, de terrain, de sismologie et de gravimétrie, Thèse de Doctorat, Université Pierre et Marie Curie, Paris VI, 356 pp.

Houseman, G., Molnar, P., 1997. Gravitational (Rayleigh–Taylor) instability of a layer with non-linear viscosity and convective thinning of the lithosphere. Geophys. J. Int. 128, 125–150.

Ionov, D., O'Reilly, S.Y., Griffin, W.L., 1998. A geotherm and lithospheric section for central Mongolia (Tariat region). Am. Geophys. Union Geodyn. Ser. 27, 127–153.

Kachanov, L.M., 1971. Foundations of the Theory of Plasticity. North-Holland, Amsterdam, 252 pp.

Kazmin, V.G., 1991. The position of continental flood basalts in rift zones and its bearing on models of rifting. Tectonophysics 199, 375–387.

Kiselev, A.I., 1987. Volcanism of the Baikal rift zone. Tectonophysics 143, 235–244.

Kiselev, A.I., Popov, A.M., 1992. Asthenospheric diapir beneath the Baikal rift: petrological constraints. Tectonophysics 208, 287–295.

Kohlstedt, D.L., Evans, B., Mackwell, S.J., 1995. Strength of the lithosphere: constraints imposed by laboratory experiments. J. Geophys. Res. 100, 17587–17602.

Kuzmin, M.I., Karabanov, E.B., Prokopenko, A.A., Gelety, V.F., Antipin, V.S., Williams, D.F., Gvozdkov, A.N., 2000. Sedimentation processes and new age constraints on rifting stages in Lake Baikal: results of deep-water drilling. Int. J. Earth Sci. 89 (2), 183–192.

Larroque, C., Ritz, J.-F., Stéphan, J.-F., San'kov, V., Arjannikova, A., Calais, E., Déverchère, J., Loncke, L., 2001. Interaction compression-extension à la limite Mongolie–Sibérie: analyse préliminaire des déformations récentes et actuelles dans le bassin de Tunka. C. R. Acad. Sci., Paris 332, 177–184.

Lesne, O., Calais, E., Déverchère, J., 1998. Finite element modelling of crustal deformation in the Baikal rift zone: new insights into the active–passive debate. Tectonophysics 289, 327–430.

Lesne, O., Calais, E., Déverchère, J., Chéry, J., Hassani, R., 2000. Dynamics of intracontinental extension in the North Baikal Rift from two-dimensional numerical deformation modelling. J. Geophys. Res. 105, 21727–21744.

Logatchev, N.A., Florensov, N.A., 1978. The Baikal system of rift valleys. Tectonophysics 45, 1–13.

Logatchev, N.A., Zorin, Yu.A., 1987. Evidence and causes of the two-stage development of the Baikal rift. Tectonophysics 143, 225–234.

Logatchev, N.A., Zorin, Yu.A., 1992. Baikal rift zone: structure and geodynamics. Tectonophysics 208, 273–286.

Logatchev, N.A., Zorin, Yu.A., Rogozhina, V.A., 1983. Baikal rift: active or passive? Comparison of the Baikal and Kenya rift zones. Tectonophysics 94, 223–240.

Lysak, S.V., 1995. Terrestrial heat and temperatures in the upper crust in South-East Siberia. Bull. Cent. Rech. Explor. Prod. Elf-Aquitaine 19, 39–57.

Malkin, B.V., Ivanchenko, G.M., 1983. On possibility of plastic failure theory: implications in analyses of the structure and seismicity of Mid-Oceanic ridges. Okeanologiya 23, 990–996 (in Russian).

Malkin, B.V., Shemenda, A.I., 1991. Mechanism of rifting: considerations based on results of physical modelling and on geological and geophysical data. Tectonophysics 199, 193–210.

Martinod, J., Davy, Ph., 1992. Periodic instabilities during compression or extension of the lithosphere: 1. Deformation modes from an analytical perturbation method. J. Geophys. Res. 97, 1999–2024.

Mattauer, M., Matte, Ph., Olivet, J.-L., 1999. A 3D model of India–Asia collision at plate scale. C. R. Acad. Sci., Paris 328, 499–508.

McClay, K.R., White, M.J., 1995. Analogue modelling of orthogonal and oblique rifting. Mar. Petrol. Geol. 12, 137–151.

McKenzie, D., 1986. The geometry of propagating rifts. Earth Planet. Sci. Lett. 77, 176–186.

Melnikov, A.I., Mazukabzov, A.M., Sklyarov, E.V., Vasiljev, E.P.,

1994. Baikal rift basement: structure and tectonic evolution. Bull. Cent. Rech. Explor. Prod. Elf-Aquitaine 18, 99–122.

Morgan, P., Baker, B.H., 1983. Introduction—processes of continental rifting. Tectonophysics 94, 1–10.

Nadai, A., 1950. Theory of Flow and Fracture of Solids, vol. 1, 2nd ed. McGraw-Hill, New York.

Olsen, K.H., 1995. Continental Rifts: Evolution, Structure, Tectonics. Elsevier, Amsterdam ILP Programme Publ. 264, 466 pp.

Petit, C., Déverchère, J., Houdry, F., Sankov, V.A., Melnikova, V.I., Delvaux, D., 1996. Present-day stress field changes along the Baikal rift and tectonic implications. Tectonics, 1171–1191.

Petit, C., Koulakov, I.Yu., Déverchère, J., 1998. Velocity structure around the Baikal rift zone from teleseismic and local earthquake traveltimes and geodynamic implications. Tectonophysics 296, 125–144.

Popov, A.M., 1990. A deep geophysical study in the Baikal region. Pure Appl. Geophys. 134 (4), 575–587.

Puzyrev, N.N., Mandelbaum, M.M., Krylov, S.V., Mishenkin, B.P., Petrik, G.V., Krupskaya, G.V., 1978. Deep structure of the Baikal and other continental rift zones from seismic data. Tectonophysics 45, 15–22.

Qayyum, M., Lawrence, R.D., Niem, A.R., 1997. Discovery of the Paleo-Indus delta–fan complex. J. Geol. Soc. London 154, 753–756.

Ranalli, G., 2000. Rheology of the crust and its role in tectonic reactivation. J. Geodynamics 30, 3–15.

Ranalli, G., Murphy, D.C., 1987. Rheological stratification of the lithosphere. Tectonophysics 132, 281–295.

Rasskazov, S.V., 1994. Magmatism related to the Eastern Siberia Rift System and the geodynamics. Bull. Cent. Rech. Explor. Prod. Elf-Aquitaine 18, 437–452.

Ritzwoller, M.H., Levshin, A.L., 1998. Eurasian surface wave tomography: group velocities. J. Geophys. Res. 103, 4839–4878.

Ruppel, C., 1995. Extensional processes in continental lithosphere. J. Geophys. Res. 100, 24187–24215.

San'kov, V.A., Miroshnichenko, A.I., Levi, K.G., Lukhnev, A.V., Melnikov, A.I., Delvaux, D., 1997. Cenozoic stress field evolution in the Baikal rift zone. Bull. Cent. Rech. Explor. Prod. Elf-Aquitaine 21, 435–455.

San'kov, V.A., Déverchère, J., Gaudemer, Y., Houdry, F., Filippov, A., 2000. Geometry and rate of faulting in the North Baikal rift, Siberia. Tectonics 19 (4), 707–722.

Schlupp, A., 1996. Neotectonic of western Mongolia using field, seismological and remote sensing data. PhD thesis, 270 pp. (in French).

Sengör, A.M.C., Nattal'in, B.A., Burtman, V.S., 1993. Evolution of the Altaid tectonic collage and Palaeozoic crustal growth in Eurasia. Nature 364, 299–307.

Shemenda, A.I., 1984. Some regularities of lithosphere deformation under tension (based on the physical modelling). USSR Acad. Sci. Rep. 275 (2), 346–350 (in Russian).

Shemenda, A.I., 1994. Subduction: Insights from Physical Modelling. Kluwer Academic Publishers, Netherlands. Ser. Modern Approaches in Geophysics, 215 pp.

Shemenda, A.I., Grokholsky, A.L., 1991. A formation and evolution of overlapping spreading centres (constrained on the basis of physical modelling). Tectonophysics 199, 398–404.

Shemenda, A.I., Groholsky, A.L., 1994. Physical modeling of slow spreading. J. Geophys. Res. 99, 9137–9153.

Sherman, S.I., 1992. Fault and tectonic stresses of the Baikal rift zone. Tectonophysics 208, 297–307.

Sherman, S.I., Gladkov, A.S., 1999. Fractals in studies of faulting and seismicity in the Baikal rift zone. Tectonophysics 308, 133–142.

Tapponnier, P., Molnar, P., 1979. Active faulting and Cenozoic tectonics of the Tien Shan, Mongolia and Baykal regions. J. Geophys. Res. 84, 3425–3459.

ten Brink, U.S., Taylor, M.H., 2002. Crustal structure of central Lake Baikal: insights into intracontinental rifting. J. Geophys. Res. 107, 10.1029/2001 JB000300.

Tommasi, A., Vauchez, A., Daudré, B., 1995. Initiation and propagation of shear zones in a heterogeneous continental lithosphere. J. Geophys. Res. 100, 22083–22101.

Tron, V., Brun, J.P., 1991. Experiments on oblique rifting in brittle–ductile systems. Tectonophysics 188, 71–84.

Vauchez, A., Barruol, G., Tommasi, A., 1997. Why do continents break up parallel to ancient orogenic belts? Terra Nova 9, 62–66.

Vauchez, A., Tommasi, A., Barruol, G., 1998. Rheological heterogeneity, mechanical anisotropy and deformation of the continental lithosphere. Tectonophysics 296, 61–86.

Villaseñor, A., Ritzwoller, M.H., Levshin, A.L., Barmin, M.P., Engdahl, E.R., Spakman, W., Trampert, J., 2001. Shear velocity structure of central Eurasia from inversion of surface wave velocities. Phys. Earth Planet. Int. 123, 169–184.

Windley, B.F., Allen, M.B., 1993. Mongolian Plateau: evidence for a late Cenozoic mantle plume under central Asia. Geology 21, 295–298.

Ziegler, P.A., 1992. Plate tectonics, plate moving mechanisms and rifting. Tectonophysics 215, 9–34.

Zonenshain, L.P., Savostin, L.A., 1981. Geodynamics of the Baikal rift zone and plate tectonics of Asia. Tectonophysics 76, 1–45.

Zorin, Y.A., 1981. The Baikal rift: an example of the intrusion of asthenospheric material into the lithosphere as the cause of disruption of the lithosphere plates. Tectonophysics 73, 91–104.

Zorin, Y.A., 1999. Geodynamics of the western part of the Mongolia–Okhotsk collisional belt, Trans-Baikal region (Russia) and Mongolia. Tectonophysics 306, 33–56.